
Volume 1 | Number 1 | Jan 2013 | Pages 1–100
NJC
New Journal of Chemistry
www.rsc.org/njc
A journal for new directions in chemistry
ROYAL SOCIETY OF CHEMISTRY
cnrs

NJC

LETTER

Fullerene Stabilized Gold Nanoparticles†

Md Tariqul Islam[a], Sudheer K. Molugu[a], Peter H. Cooke[b], Juan C. Noveron*[a]

Received 00th January 20xx,
Accepted 00th January 20xx

DOI: 10.1039/x0xx00000x

www.rsc.org/

We report a simple and one-step method of generating gold nanoparticles stabilized directly with fullerenes C_{60} and [6,6]-phenyl-C_{61}-butyric acid (PCBA) that led to C_{60}-AuNPs (1) and PCBA-AuNPs (2), respectively. The C_{60}-AuNPs (1) and PCBA-AuNPs (2) were characterized with UV-Vis, FTIR, DLS, Zeta potential, XRD, TEM, and AFM.

Fullerene assemblies on metal surfaces have received much attention both experimentally[1] and theoretically.[2] In particular, the binding of C_{60} on to the Au(111) surface lattice has been found to be very strong[1,3] with binding energy calculated to be about 200 kJ/mol,[2] which is higher than the gold-sulfur bond strength of 187 kJ/mol.[4] Monolayer assemblies of C_{60} on to gold surfaces have been demonstrated to exhibit intriguing properties including electrochemical sensing,[5] catalysis,[6] and light harvesting,[7]. Mechanistic studies of the formation of the C_{60} monolayer on the Au(111) indicates that C_{60} nucleates at the steps separating narrow terraces of the crystal surface followed by growth from the steps onto the larger terraces.[8] Moreover, an experimental study showed that C_{60} and the Au(110) surface exhibit an adsorption energy of 1.09 eV through van der Waals interactions**.**[9] However, it has been suggested that the monolayer adsorption of C_{60} on metal surfaces also involve chemical bonding originated from the charge transfer and LUMO-metal state mixing that form the LUMO-metal hybrid states.[1]

Direct binding of fullerene C_{60} on the surface of gold nanoparticles (AuNP) have not been reported to date, to the best of our knowledge. However, there have been reports of fullerenes anchored to gold nanoparticles via functional groups such as thiol,[10-12] and bipyridyl groups.[13] Fullerenes have also been incorporated on AuNPs by mediation with third party molecules such as didodecyldimethylamonium bromide,[14] dodecylamine,[15] and thiol-containing porphyrins[16] that can anchor the fullerenes. Similarly, gold nanoparticles have also been deposited on to the surface of C_{60} microcrystals.[17]

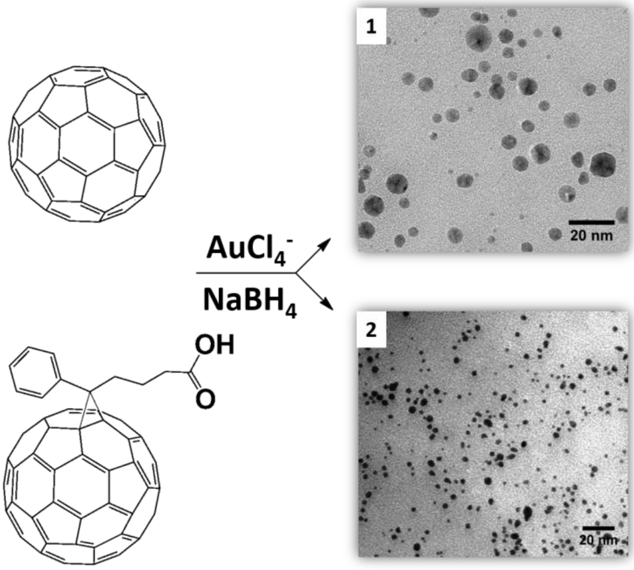

Figure 1. Synthesis of C_{60}-AuNPs (**1**) and PCBA-AuNPs (**2**).

Herein we report for the first time the stabilization of AuNPs directly with fullerenes possibly via the multiple binding modes of fullerenes demonstrated on gold surfaces and the van der Waals interactions, which are also observed between AuNPs and bis(phthalocyaninato)lanthanide(III) complexes.[18] The synthesis and characterization of C_{60} and [6,6]-phenyl-C61-butyric acid (PCBA) leading to C_{60}-AuNPs (**1**) and PCBA-AuNPs (**2**), respectively, is reported. The C_{60}-AuNPs (**1**) makes a very stable burgundy color solution in DMF or a mixture of DMF and water whereas the latter one makes brown solutions in water as well as methanol under ambient condition, Figure 1. The C_{60}-AuNPs (**1**) and PCBA-AuNPs (**2**) were characterized with UV-Vis, FTIR, DLS, zeta potential, XRD, TEM, and AFM.

The C_{60}-AuNPs (**1**) and PCBA-AuNPs (**2**) were prepared by dissolving $HAuCl_4{\cdot}3H_2O$ and the fullerenes in a mixture of solvents

---

[a] Department of Chemistry, University of Texas, El Paso, 500 West University Avenue, El Paso, Texas 79968, USA
[b] CURRL, New Mexico State University, 945 College Dr., Las Cruces, NM 88003, USA

†Electronic Supplementary Information (ESI) available: [FTIR, TEM images, XRPD, DLS, and Zeta-potential measurements. This material is available free of charge via the Internet at http://pubs.acs.org.
]. See DOI: 10.1039/x0xx00000x

consisting of DMF, toluene and/or 1,2-Dichlorobenzene followed by addition of a methanolic $NaBH_4$ solution with vigorous stirring at room temperature. The same reaction in the absence of fullerenes resulted in purple gold nanoparticles that immediately lump into insoluble metallic gold aggregates driven by inter-nanoparticle core fusion.

UV-vis spectra of C_{60}-AuNPs (**1**) and PCBA-AuNPs (**2**) are shown in Figure 2. The UV-vis absorption spectrum of C_{60}-AuNPs (**1**) in DMF shows a strong absorption band centered at 527 nm, which is the characteristic surface-plasmon resonance absorption band that is usually observed for gold nanoparticles.

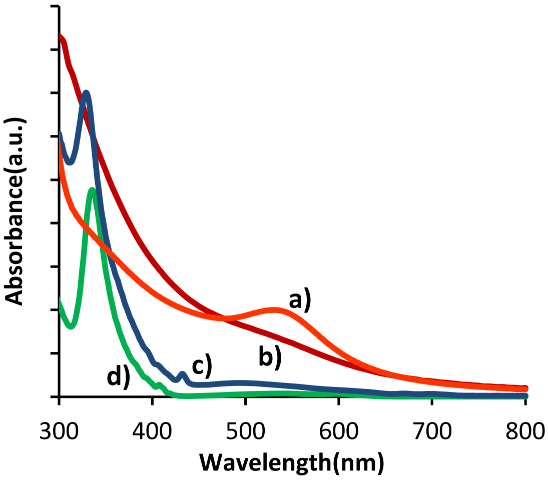

Figure 2. UV-Vis absorption spectra of a) C_{60}-AuNPs (**1**) in DMF, b) PCBA-AuNPs (**2**) in water c) PCBA in DMF and d) C_{60} in toluene.

However, the PCBA-AuNPs (**2**) in water has a broad and weak absorption band extending between 500 – 550 nm, which is the characteristic surface-plasmon absorption band for gold nanoparticles having very small size,[10] nearly 2 nm in size.[19] The absence of clear surface-plasmon absorption band in PCBA-AuNPs (**2**) could have happened because of the aggregation of the nanoparticles. Aggregation of the PCBA-AuNPs (**2**) was observed in TEM as well as DLS analysis,(See supporting information). We also observed the absence of the characteristic absorption bands of C_{60} at 334 nm and 405 nm and for PCBA at 328 nm and 431 nm. This indicates the fullerene C_{60} and PCBA underwent some addition reactions forming fullerene derivatives which we do not understand yet completely. Addition reactions on fullerene cage usually show this type of phenomenon as a result of the loss of the π-π conjugation through the cage.

The size, shape, and dispersity of C_{60}-AuNPs (**1**) and PCBA-AuNPs (**2**) were examined by using the Transmission Electron Microscopy (TEM) and High-Resolution-TEM (HR-TEM), Figure 3. TEM of C_{60}-AuNPs (**1**) shows that the AuNPs are mostly individual and have a range of core diameters from 1.5 to 15 nm and an average of 3.04 nm. The TEM of PCBA-AuNPs (**2**) shows nanoparticles with core diameters ranging from 1.6 to 6.5 nm and an average of 3.2 nm, (See supporting information for more TEM images). HR-TEM studies on C_{60}-AuNPs (**1**) and PCBA-AuNPs (**2**) revealed AuNPs with a fcc crystalline gold lattice at their core. The interlayer spacing measured at about 0.23 nm is characteristic of the lattice space of Au(111) planes.[20]

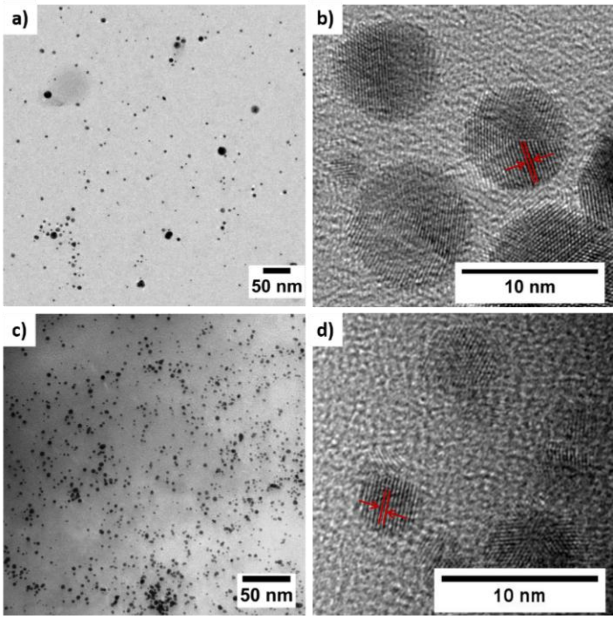

Figure 3. a) TEM and b) HR-TEM of C_{60}-AuNPs (**1**),c) TEM and d) HR-TEM of PCBA-AuNPs (**2**). HR-TEM images show in red the interlayer spacing of 0.23 nm, which is characteristic of the Au (111) lattice planes.

Atomic Force Microscopy (AFM) of C_{60}-AuNPs (**1**) and PCBA-AuNPs (**2**) was conducted on freshly cleaved mica to reveal the particle morphology of the AuNPs, Figure 4. AFM revealed that the AuNPs exist as homogenously dispersed individual nanoparticles similar in size to those shown in the HR-TEM images. Vertical analysis of two particles is shown in Figure 4(b & d).

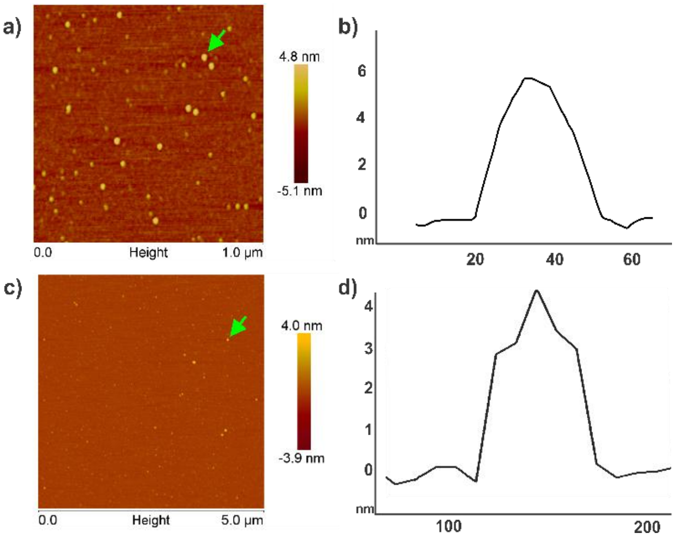

Figure 4. AFM images of a) C_{60}-AuNPs (**1**) and b) vertical analysis of one C_{60}-AuNP(**1**) shown in green arrow; c) AFM images of PCBA-AuNPs (**2**) and d) vertical analysis of one PCBA-AuNP (**2**) shown in green arrow.

The FTIR (see supporting information) of the C_{60}-AuNPs (**1**) shows the appearance of the alkyl C-H stretching vibrations at 2924 cm^{-1}, which is indicative that hydrogenation occurred on C_{60} cage during the formation of the nanoparticles. Moreover, the two intense C_{60} ring stretching vibrational modes at 1180 and 1427cm^{-1} known as Tu(3) and Tu(4) disappeared, probably due to the loss of symmetry of the fullerene cage. The FTIR spectrum also revealed bands located at 3380, 1056, 1390, and 1600 cm^{-1}, which are characteristic stretching vibrational mode of hydroxyl groups (O-H), the stretching mode of C-O, the bending mode of C-OH, and the stretching mode of C=C, respectively. On the other hand, the FTIR spectrum of the PCBA-AuNPs (**2**) does not reveal C-H stretching bands, but shows bands at 3380, 1072, 1389 and 1586cm^{-1}, which can be identified as the stretching vibrational mode of hydroxyl groups (O-H), the stretching mode of C-O, the bending mode of C-OH, and the stretching mode of C=C, respectively. This type of IR spectra is comparable to the one reported for C_{60} fullerenol,[21,22] and lead us to infer that some of the fullerenes bonded on the surface of the AuNPs may be hydroxylated. We believe that the formation of the fullerenol makes the nanoparticles soluble in DMF, a mixture of DMF and water, and make them insoluble in toluene, dichlorobenzene, carbondisulfide and other nonpolar solvents.

XRD spectra (see supporting information) of C_{60}-AuNPs (**1**) and PCBA-AuNPs (**2**) revealed a broad peak extended from 10^0 to 22^0 that corresponds to the amorphous carbon from the fullerenes. The characteristic face-centered cube (fcc) crystalline gold diffraction pattern was observed at $2\theta = 38.06^0$, 44.16^0, 64.22^0, and 77.5^0 corresponding to the crystalline faces of (111), (200), (220) and (311), respectively.[23] The other set of sharp peaks located at 2θ = 31.55^0, 45.30^0, 56.68^0, 65.45^0 and 75.00^0 is due to the presence of crystalline NaCl which co-precipitated out with gold nanoparticls while the addition of diethylether. This crystallized NaCl can easily be washed out with water or other polar solvents.

Dynamic light scattering (DLS) was carried out (see supporting information) to determine the size distribution profile of the particles in solution. For C_{60}-AuNPs (**1**) in DMF at a concentration sufficient to obtain high signal to noise ratio the DLS showed two particle populations with average hydrodynamic radii of 18 and 250 nm. For PCBA-AuNPs (**2**) in water, DLS revealed two particle populations with average hydrodynamic radius of 45 nm and 200 nm. These results indicate that, at these concentrations, C60-AuNPs (**1**) and PCBA-AuNPs (**2**) can form individual and aggregated dispersions of nanoparticles in solution, possibly mediated by the π-π stacking interactions between the fullerenes.

Zeta potential measurements on C_{60}-AuNPs (**1**) in a mixture of DMF and water and PCBA-AuNPs (**2**) in water (see supporting information) showed a negative value of -18 mV and -47.0 mV, respectively. This negative zeta potential means that the AuNP surface has a net negative charge, which may contribute to the high dispersion stability in solution due to the interparticle electrostatic repulsive forces. The higher negative zeta potential of PCBA-AuNPs (**2**) may be attributed to the intrinsic negative charge of [6,6]-phenyl-C_{61}-butyrate.

The exact mechanism of the functionalization of C_{60} and PCBA in C_{60}-AuNPs (**1**) and PCBA-AuNPs (**2**) is not well understood at this point. However, the very strong and well-established bond between metallic gold and fullerene indicates that the fullerene cage adsorbs onto the gold surface and stabilize the gold nanoparticles.

In conclusion, we report a simple, one-step method of generating gold nanoparticles directly stabilized with two types of fullerenes, C_{60} and [6,6]-phenyl-C_{61}-butyric acid (PCBA) leading to C_{60}-AuNPs (**1**) and PCBA-AuNPs (**2**), respectively. C_{60}-AuNPs (**1**) is soluble in DMF and a mixture of DMF and water, whereas PCBA-AuNPs (**2**) is soluble in water as well as methanol. The C_{60}-AuNPs (**1**) and PCBA-AuNPs (**2**) are the first examples of gold nanoparticles directly stabilized by fullerenes.

Experimental

Synthesis of C_{60}-AuNPs (1):

To a solvent mixture of 20 mL of toluene, it was added 5 mg (0.006944 mmol) of C_{60} and stirred and sonicated until dissolved. In another container, 10mg (.0254 mmol) $HAuCl_4 \cdot 3H_2O$ was dissolved in 20 mL DMF. Both of these solutions were mixed together with stirring. In a separatory funnel a solution prepared from10 mg (0.2643 mmol) $NABH_4$ in 10 mL of methanol was added to the above mixture in about 7 sec period of time with vigorous stirring. The stirring was continued for 24 hours at room temperature and the reaction formed a stable solution without a precipitate. Afterwards, 80 mL of diethyl ether was added to obtain a precipitate of nanoparticles that were collected by centrifugation at 5000 rpm for 10min. The isolated nanoparticles were washed twice in diethylether. We observed that the wet nanoparticles, as centrifuged after the ether wash, are very soluble in DMF and a mixture of DMF and water, but if allowed to dry at 70^0 C, they become insoluble.

Synthesis of PCBA-AuNPs (2):

To a solvent mixture consisting of 10 mL of 1,2-dichlorobenzene and 23 mL of DMF it was added 20.6 mg (.02294 mmol) PCBA and allowed to stir and sonicate until dissolved. In another container, 15 mg (.0381 mmol) of $HAuCl_4 \cdot 3H_2O$ was dissolved in 2 mL of DMF. Both of these solutions were mixed together with stirring. In a separatory funnel, a solution prepared from 16 mg (0.4229 mmol) of $NABH_4$ in 10 mL of methanol was added into the above solution drop wise with vigorous stirring in about 3 min. of time period. The stirring was continued for 24 hours at room temperature and the reaction formed a stable solution without a precipitate. Afterwards, 80 mL of diethyl ether was added and generated a precipitate of the nanoparticles that was collected by centrifugation at 5000 rpm for 10min. The isolated nanoparticles were washed twice in diethylether and dried at room temperature. The dry nanoparticles were found to be fairly soluble in water and methanol.

Acknowledgement

Financial support from NSF grants DMR PREM-1025302, MRI-0923437, CHE-0748913, and USDA 2014-38422-22078 are gratefully acknowledged.

Notes and references

Department of Chemistry, University of Texas, El Paso, 500 West University Avenue, El Paso, Texas 79968, USA.
Dr. Juan C. Noveron; E-mail: jcnoveron@utep.edu

1 T. R. Ohno, Y. Chen, S. E. Harvey, G. H. Kroll, J. H. Weaver, R. E. Haufler, Smalley, R. E. Smalley, *Phys. Rev. B*. 1991, **44**, 13747.
2 G. J. Bubnis, S. M. Cleary, H. R. Mayne, *Chem. Phys. Lett*. 2009, **470**, 289.
3 A. Kuzume, E. Herrero, J. M. Feliu, R. J. Nichols, D. J. Schiffrin, *Phys. Chem. Chem. Phys.*2004, **6**, 619.
4 B. Bhushan "Springer Handbook of Nanotechnology," 3rd Edition, Springer, Berlin, **2010**.
5 R. N. Goyal, V. K. Gupta, N. Bachheti, R. A. Sharma, *Electroanalysis*. 2008, **20**, 757.
6 C. Roth, I. Hussain, M. Bayati, R. J. Nichols, D. J. Schiffrin, *Chem.Commun.* 2004, **13**, 1532.
7 H. Imahori, H. Norieda, H. Yamada, Y. Nishimura, I. Yamazaki, Y. Sakata, S. Fukuzumi, *J.Am. Chem Soc.* 2001, **123**, 100.
8 E. I. Altman, R. J. Colton, *Surf. Sci.* 1992, **279**, 49.
9 C. Chavy, C. Joachim, A. Altibelli, *Chem. Phys. Let.*1993, **214**, 569.
10 P. K. Sudeep, B. I. Ipe, K. G. Thomas, M. V. George, S. Barazzouk, S. Hotchandani, P. V. Kamat, *Nano Lett.* 2002, 2, 29.
11 Y. S. Shon, H. Choo, *Chem. Commun.* 2002, **21**, 2560.
12 P. Piotrowski, J. Pawłowska, J. Pawłowski, A. Więckowska, R. Bilewicz, A. Kaim, *J. Mat. Chem. A.* 2014, **2**, 2353.
13 C. Du, B. Xu, Y. Li, C. Wang, S. Wang, Z. Shi, D. Zhu, *New J. Chem.* 2001, **25**, 1191.
14 M. Brust, C. J. Kiely, D. Bethell, D. J. Schiffrin, *J. Am. Chem. Soc.* 1998, **120**, 12367.
15 V. Yong, H. T. Hahn, *Adv. Nanoparticles*, 2013, **2**, 1.
16 T. Hasobe, H. Imahori, P. V. Kamat, S. Fukuzumi, *J. Am. Chem. Soc.*, 2003, **125**, 14962.
17 Z. Tan, A. Masuhara, S. Ohara, H. Kasai, H. Nakanishi, H. Oikawa, *J. Nanoparticle Res.*2013, **15**, 1.
18 Y. Noda, S. I. Noro, T. Akutagawa, T. Nakamura, *Sci. Rep.*2014, **4**,1.
19 F. Deng, Y. Yang, S. Hwang, Y. S. Shon, S. Chen, *Anal. Chem*. 2004, **76**, 6102.
20 S. Singh, R. Pasricha, U. M. Bhatta, P. V. Satyam, M. Sastry, B. L. V. Prasad, *J. Mat. Chem.* 2007, **17**, 1614.
21 K. Kokubo, K. Matsubayashi, H. Tategaki, H. Takada, T. Oshima, *ACS Nano.* 2008, **2**, 327.
22 Y. B. Sun, C. Y. Cao, S. L. Yang, P. P. Huang, C. R. Wang, W. G. Song, *Chem. Commun.* 2014, **50**, 10307.
23 X. Feng, J. Hu, X. Chen, J. Xie, Y. Liu, *J. Phys. D: Appl. Phys*. **2009**, 42, 042001.